Proceedings World Geothermal Congress 2020+1
Reykjavik, Iceland, April - October 2021

Including Seismic Risk Mitigation Measures into the LCOE in EGS for Optimal Siting

Dimitrios Karvounis, Arnaud Mignan, Marco Broccardo, Stefan Wiemer, and Domenico Giardini

Swiss Seismological Service, ETH-Zurich, NO H 62, Sonneggstrasse 5, 8092, Zurich, Switzerland

karvounis@sed.ethz.ch

Keywords: Levelized Cost Of Electricity, Enhanced Geothermal Systems, Seismicity, Risk Mitigation, Meta-model

ABSTRACT

The risk associated with induced seismicity and the cost of mitigation strategies decrease the competitiveness of Enhanced Geothermal Systems (EGS). The most used mitigation strategy, the Traffic Light Systems (TLS), modifies or eventually stops reservoir stimulations as a function of the induced seismic risk. Despite the significant economic consequences of such actions, the direct and indirect costs of TLSs have not been included yet in the Levelized Cost of Electricity (LCOE). In this work, we systematically fill this gap by introducing an analytical geothermal energy model, which evaluates and updates the optimal price of electricity based on TLS mitigation scenarios. The proposed model estimates the production of electricity, the heat credit, and introduces a mitigation cost during the reservoir stimulation based on the probability of dismissing the injection as a function of TLS forecasts. Moreover, during the production phase, the net energy generated is decreased by clipping the production flow rate so that the reservoir's overpressure does not exceed the regional minimum effective stress. While the mitigation cost decreases with the distance between the injection point and exposed building stocks, the operational costs increase with the same distance. Accordingly, we investigate the trade-off between heat credit and seismic risk mitigation cost for the optimal siting of EGS power plant. Finally, we introduce an optimization strategy for analyzing the potential impact of seismic safety standards in determining the number of EGS plants that can be expected in a given region.

1. INTRODUCTION

What is easier to predict? An earthquake or the geothermal power generation in 5 years from now? When it comes to induced earthquakes, the maximum induced earthquake magnitudes are consistent with the extreme value distribution arising from the classical Gutenberg-Richter frequency magnitude law (e.g. van der Elst et al., 2016). There is therefore a complete probabilistic forecasting model which has been proved to be consistent with the outcome of several projects. On the other hand, the global installed geothermal capacity grew with an annual rate 3.15% from 2010 until 2015 (Bertani, 2016), but the forecasts reported by various geothermal stakeholders to Bertani (2012) for the same 5-years period was 12.6% annual growth on average. A significant offset. In the case of Enhanced Geothermal Systems (EGS) at least, one can safely claim that forecasting the growth of EGS is a more complex task than forecasting earthquakes. Not only because this growth depends on the volatility of the energy market and social acceptance, two parameters heavily influenced by eventualities, but also because this growth depends on our ability in forecasting an eventuality such as a large induced earthquake with major consequences.

The development of EGS decelerated after the multiple Mw 3 earthquakes from the EGS at Basel, Switzerland in 2006 (Giardini, 2009) and at St Gallen, Switzerland in 2013 (Edwards et al., 2015). Further deceleration is likely going to happen now that damages from the Mw 5.5 earthquake in 2017 due to the EGS at Pohang, South Korea seem to outbalance any realistic revenue one could expect from an EGS power plant (Lee et al., 2019). In hindsight, it is clear that some of the past EGS projects would have gained from better management of injection-induced seismicity risk given their proximity to large cities with maximal exposure (Lee et al., 2019). The state-of-the-art in managing the risk from induced seismicity are the risk-based Traffic Light Systems (TLS) that reassess and forecast the risk in time for the operators to avoid potentially dangerous situations. Their development started before the EGS in Pohang (Mignan et al., 2015; Baker and Gupta, 2016), but without a risk-based one being employed there (Lee et al., 2019). Given that a successful EGS can happen only after a successful stimulation with sufficiently many benign seismic events between the wells, it is now the general consensus that EGS cannot grow without risk-based TLS and without the stakeholders abiding by the TLS protocols.

Binding the growth of EGS with TLS should not cast doubts about the technology's potential. EGS remains one of the very few renewable and carbon-free technologies that can mass-produce robustly and securely both electricity and heat, and without being limited to volcanic countries. The sector of electricity and heat is the most carbon-emitting sector in the global energy mix and is expected only to grow as our digital needs for base-load energy increase (Andrae and Edler, 2015). Several states have high hopes of EGS assisting in the decarbonizing of this sector and both fundamental and applied research is extensively funded and performed in an effort of improving both the safety and the commerciality of EGS (Amann et al., 2018; Kneafsey et al., 2018). A necessary but now missing step towards making EGS competitive is allowing EGS stakeholders to confidently estimate the return of investment in light of the necessity for risk-based TLS.

Here, the key points and their implications are analyzed for our work published in Mignan et al. (2019). There, the effect that abiding by TLS has in the Levelized Cost of Electricity (LCOE) is studied and the new most cost effective distance of an EGS site from urban environments is estimated. It is also shown, how both the new LCOE and the optimal distance can be affected by induced seismicity during the production phase, because of which seismicity significant limits to the production rate may be required.

In section 2, a meta-model that allows quick but realistic estimations of the LCOE without TLS is presented, where the LCOE depends on design choices (e.g. number, diameter, and depths of wells), on physical properties (e.g. type of injected fluid and

produced temperature), and of the site's distance from the market to which the waste heat can be sold. In section 3, a risk-based protocol for TLS is described, which protocol depends on the exposure of the EGS and stimulation's design choices (i.e. total injected volume), and the meta-model for LCOE is extended to include both the protocol and the expected behavior of EGS stakeholders while operating the TLS. In section 4, the meta-model is employed for finding the optimal siting of EGS in a free-market scenario and the maximum installed capacity of a region with known exposure. Finally, conclusions are discussed in section 5.

Both the work presented and the bibliographical background of it are thoroughly explained by Mignan et al. (2019). All figures have been adapted from the same publication. See also Mignan et al. (2019b) for a perspective from a risk governance point of view.

2. ENHANCED GEOTHERMAL SYSTEM META-MODEL

Typically, an EGS is expected to be developed only when it can provide further electricity to the market at a competitive price and safely. When induced seismicity considerations are neglected, then the LCOE can be approximated with the price value

$$P_{EGS} = \frac{C}{E}, \tag{1}$$

where E is the total amount of energy revenue, C the costs required for generating E, and annuity is neglected. In the subsections that follow, a meta-model is described that allows approximating analytically an upper bound of possible E, both for electricity and heating, and based on this upper bound a meaningful lower bound of P_{EGS} can be assessed.

Unless explicitly written, SI units are considered for all variables considered here.

2.1 Energy system for modeling the upstreaming and the downstreaming of geothermal energy

Total commercial energy revenues E from an EGS are approximated here as

$$E = \left(E_{el} + r_{market} E_{DH}\right) \Delta t_{life}, \tag{2}$$

where Δt_{life} is the life expectancy of an EGS power plant, r_{market} is the ratio between the prices of electricity and heating, and E_{el} and E_{DH} are the mean electrical power and heat, respectively, that downstream from the EGS to the energy market over the life expectancy of the EGS.

In order to approach a realistic upper bound for E, a simplified energy system is considered (Fig. 1) and analytical expressions of the maximum values both for E_{el} and E_{DH} are derived. In the considered energy system, geothermal heat E_{th} is first upstreamed from depth Z and then delivered to the conversion cycle of the EGS, without unintended seismicity. In the conversion cycle, a portion η_{el} of the upstreamed energy is converted to electricity and the remaining heat is available for direct utilization (e.g. heating a local community). The operational needs of the EGS in electricity W_{EGS} are covered from its own production and are not included in E_{el}. The available waste heat can be directly utilized by the nearest communities that already operate a district heating system and at distance L. Heat is supplied to this community through supply and return pipes, where each pipe is of length L and none is perfectly isolated.

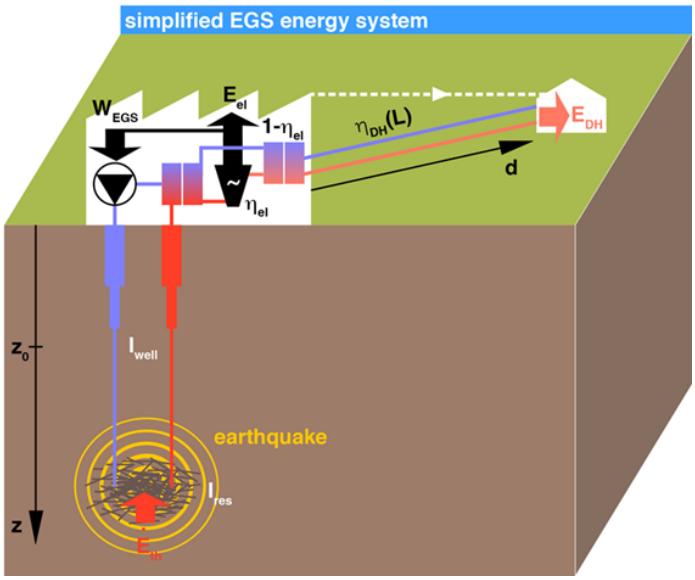

Figure 1: A simplified EGS energy system consisting of three cycles is depicted, i.e., a) an EGS power plant upstreams energy E_{th} from a depth Z while consuming energy W_{EGS}, b) a conversion cycle that converts a portion η_{el} of E_{th} to electricity, and c) a pipe of length $L \geq d$ that supplies a remote community at distance d with the waste heat and with efficiency η_{DH}. Source: Mignan et al., 2019

2.1.1 Maximum generated electricity

The only operational need considered here is the energy required by the pumps at the wells of the EGS. The energy consumed by the pumps compensates for the linear pressure losses of the working fluid along the reservoir ΔP_{res} and for the non-linear pressure losses in the wells ΔP_{wells}. Also, a positive thermosiphon gain due to gravitational effects ΔP_g is considered, which reduces this operational need of the EGS. At any moment, the electrical energy that the EGS provides to the market is approximated as

$$E_{el} = \eta_{el} E_{th} - \overbrace{V_{inj}(\Delta \mathrm{P}_{res} + \Delta \mathrm{P}_{well} - \Delta \mathrm{P}_g)}, \tag{3}$$

where V_{inj} is the injected flow rate, an ideal pump is considered, and the equation suggested by Zarrouk and Moon (2014)

$$\eta_{el} = 0.078795 \cdot \ln\left(h_{prod}\right) - 1.00081 \tag{4}$$

is a good fit for the conversion efficiency of EGS, where h_{prod} is the enthalpy of the produced water.

Each of the remaining terms in eq. (3) is modeled as

$$\begin{cases} E_{th} &= V_{inj}\rho_{inj}c_w\Delta T \\ \Delta \mathrm{P}_{res} &= \dfrac{I_{res}}{N_{res}} V_{inj} \\ \Delta \mathrm{P}_{well} &= I_{well} V_{inj}^{1.75} \\ \Delta \mathrm{P}_g &= Zg\Delta\rho \end{cases} \tag{5}$$

where ρ_{inj} is the density of the injected fluid, c_w is the fixed specific heat capacity, ΔT the difference between the produced and the injected temperature for the fluid, I_{res} is the reservoir impedance after a successful stimulation, N_{res} is the number of independent and identical flow paths (e.g., $N_{res}=1$ for doublets, 2 for triplets, …), I_{well} is the total of wells' impedances for turbulent flow, and g is the gravitational acceleration.

Note that the exponent 1.75 used for modeling ΔP_{well} is because of the empirical Blasius fit that is considered for approaching the Darcy's friction in a pipe with turbulent flow, and hence the pressure drop per meter of the pipe equals

$$\frac{dP}{dl} \approx 0.241 \cdot \frac{\rho^{0.75}\mu^{0.25}}{D^{4.75}} \cdot V^{1.75}, \tag{6}$$

where D is the diameter of the pipe and μ the viscosity of the fluid. The total impedance of the system of wells I_{well} can then be approximated through the harmonic average of the elementary parts of the wells.

By combining eqs. (3)-(6), the rate V_{opt} that maximizes the commercially exploitable electricity is the solution of the equation

$$0 = -2.75 \cdot I_{well} \cdot V_{opt}^{1.75} - 2\frac{Ires}{Nres} V_{opt} + \left(\eta_{el}\rho_{inj}c_w\Delta T + \Delta \mathrm{P}_g\right), \tag{7}$$

the solution of which is approximately equal to

$$V_{opt} \approx \left(\frac{\left(2\dfrac{Ires}{Nres}\right) \pm \sqrt{\left(2\dfrac{Ires}{Nres}\right)^2 - 11 \cdot I_{well} \cdot \left(\eta_{el}\rho_{inj}c_w\Delta T + \Delta \mathrm{P}_g\right)}}{5.5 \cdot I_{well}} \right) + \left(\frac{B_1 \pm \sqrt{B_1^2 - 4 \cdot A_1 \cdot C_1}}{2 \cdot A_1} \right), \tag{8}$$

where the first term in parenthesis is the solution of the quadratic form of eq. (7), and the second is its correction with

$$\begin{cases} A_1 &= -1.8047 \cdot I_{well} \cdot V_0^{-0.25} \\ B_1 &= -4.8125 \cdot I_{well} \cdot V_0^{0.75} - 2\dfrac{I_{res}}{N_{res}} \\ C_1 &= -2.75 \cdot I_{well} \cdot V - 2\dfrac{I_{res}}{N_{res}} \cdot V + \left(\eta_{el}\rho_{inj}c_w\Delta T + \Delta \mathrm{P}_g\right) \end{cases} . \tag{9}$$

The meta-model considers $E_{el}(V_{opt})$ as the maximum electrical revenue and its value depends only on $\{Z, \Delta T, T_{inj}, I_{well}, (I_{res}/N_{res})\}$. In Fig. 2 (top row), electrical revenue and their $E_{el}(V_{opt})$ are plotted for three exemplary EGS designs, i.e. a doublet, a doublet with 3 stages, and a triplet), for wells similar to the well in Basel, $I_{res} = 2$ MPa/(l/s), $T_{inj} = 65$°C and a steady increase of ΔT with Z.

2.1.1 Direct usage of waste heat from nearby communities

Out of the $(1-\eta_{el})\dot{E}_{th}$ heat available for direct utilization, a portion will be lost to the environment due to the imperfect insulation of the supply pipe. An exponential decline is assumed for the heat losses along the supply pipe and also a minimum temperature is required at the exit of the supply pipe for it to be commercially interesting. In this case, the total heat sold for direct utilization is found equal to

$$E_{DH}=\begin{cases} 0 & \text{, if } E_{th}<\dfrac{eUL\Delta T_{\min}}{(1-\eta_{el})} \text{ or } V_{inj}<\dfrac{UL}{cW_0\left(\dfrac{UL\Delta T_{\min}}{(1-\eta_{el})E_{th}}\right)} \\ (1-\eta_{el})E_{th}\exp\left(W_0\left(-\dfrac{UL\Delta T_{\min}}{(1-\eta_{el})E_{th}}\right)\right) & \text{, otherwise } (W_0 \text{ is the main branch of the Lambert eq.}) \end{cases} \quad (10)$$

where U is the insulation value of the pipe, L is the length of the supply pipe, $\Delta T_{\min}$ the minimum acceptable temperature difference from the ground's temperature at the end of the supply's pipe, and W_0 is the principal branch of the Lambert function. Practically, the waste heat of the EGS returns profit neither when it is little nor when the EGS circulates at a very low rate.

The maximum amount of heat that can be offered for direct usage is the value of E_{DH} for V_{opt}.

In Fig. 2 (bottom), the maximum distance at which waste heat with temperature at least ΔT_{min} larger than the ground's temperature is plotted as well as the maximum amount of commercially exploitable heat that the EGS can provide for different operational depths, where $\Delta T_{min}=35°C$.

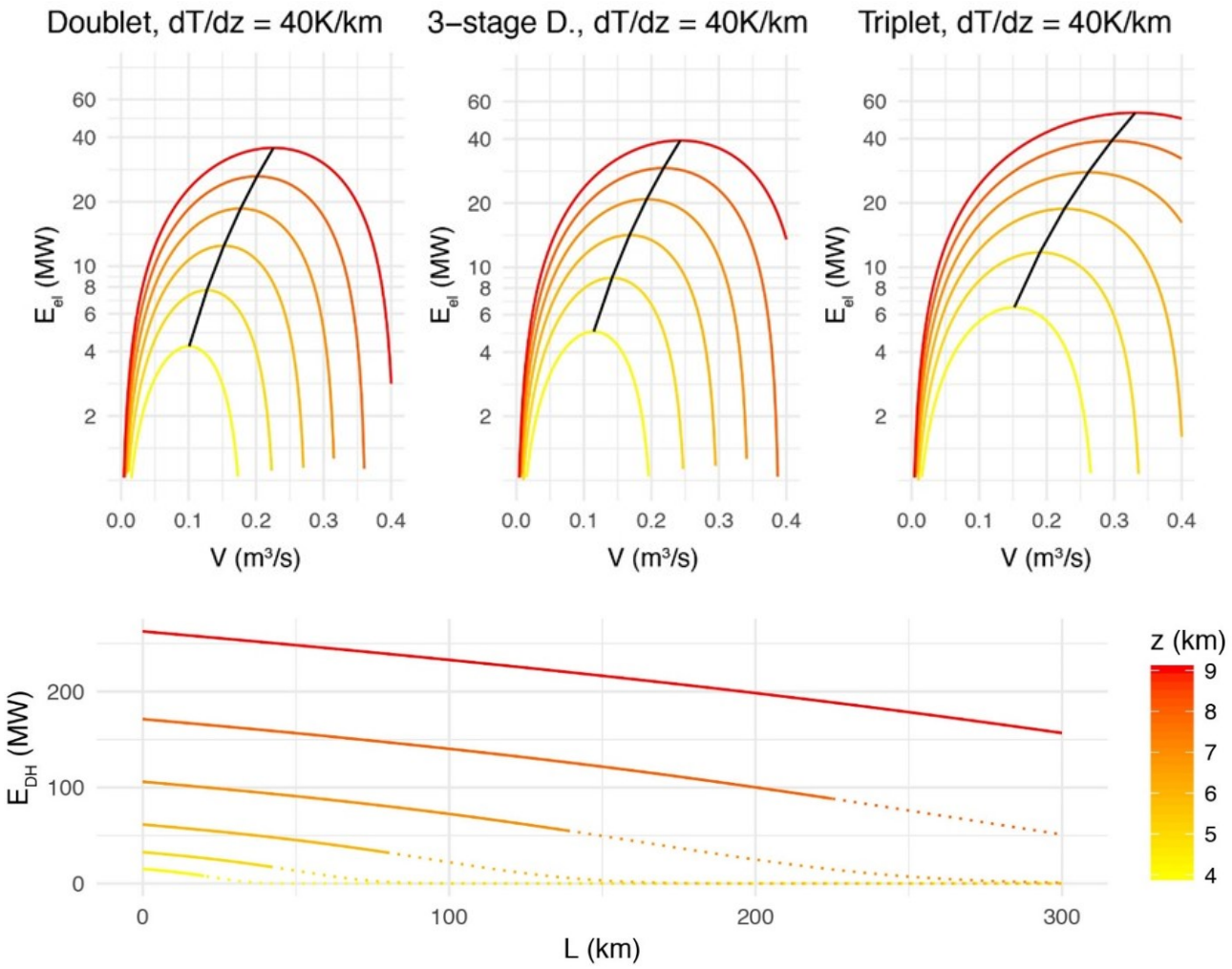

Figure 2: On top, the relationship between injected flow rate and electrical power is plotted for three different EGS scenarios, as well as the flow rate that maximizes power revenue (black curve). On the bottom, the commercially exploitable heat of the district heating model is plotted for the triplet's V_{opt} and as a function of pipeline length L between the power plant and an existing heat district. Source: Mignan et al., 2019

2.2 Costs of EGS

Necessary costs for constructing an operational EGS power plant that sells both electricity and heat are

$$C = n_{well}\left(C_{well} + C_{frac}\right) + C_{plant} + r_{renew} n_{well} C_{well} + C_{DH}\,, \tag{11}$$

where n_{well} are the wells required for E, C_{well} is the cost of well drilling, C_{frac} is a fixed cost for stimulating each well, C_{plant} is the cost of the power plant, r_{renew} is the rate of well renewal for the drilled well during the plant's lifetime Δt_{life} , and C_{DH} is the cost of constructing the supply and return pipelines connected with the district heating. Here, the possibility of an EGS well to be abandoned during stimulation is not considered, and therefore, the investment $C_{TLS} = (C_{well}+C_{frac})$ returns revenue for all wells considered. Later, the probability of this C_{TLS} investment becoming a loss due to induced seismicity will be considered.

Main dominant costs are approximated and according to bibliography as

$$\begin{cases} C_{well} & \approx & a_w\left(0.172\cdot Z^2 + 2300\cdot Z + 6.2\cdot 10^5\right) \\ C_{plant} & \approx & a_{pl}\cdot\left(0.75 + 1.125\cdot E_{el}\cdot e^{-6.115\cdot 10^{-3}\left(E_{el}-5\right)}\right), \\ C_{DH} & \approx & 840\cdot L \end{cases} \tag{12}$$

where all costs are in US $, and $1 \le a_w \le 2$ and $1 \le a_{pl} \le 2$ are two parameters treated as random. The input parameters $\{Z, \Delta T, T_{inj}, I_{well}, (I_{res}/N_{res}), a_w, a_{pl}\}$ for 10,000 scenarios are sampled, realistic fixed values are considered for $C_{frac} = US\ \$\ 10^6$ and $r_{market} = 1/3$, and the minimum LCOE is estimated for the optimum $\dot{I}_{opt}$ scenario. The 25-75% and 5-95% ribbons are plotted in Fig. 3 for all sampled scenarios, as well as the range of sampled cost properties. The ribbons of sampled costs and of estimated revenue and minimum P_{EGS} are plotted and compared to results from previous similar studies (MIT, 2006; Tester et al., 2007; Beckers et al., 2014; Hirschberg et al, 2015), both for the case where only electricity is sold (orange ribbon) and for the case where the total of the waste heat is sold for $r_{market} = 1/3$ (red ribbon).

Practically, the lower bound of the red ribbon approaches the limit at which further significant reduction of the LCOE is physically impossible for the considered conversion efficiency.

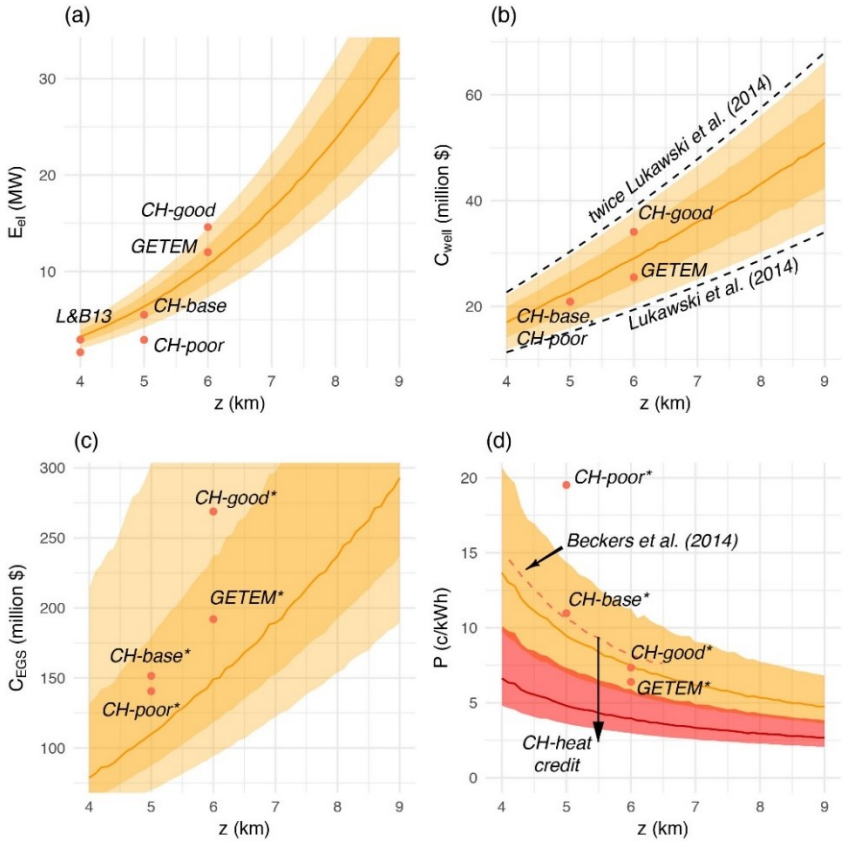

Figure 3: Economic model parameters and pricing P_{EGS} as a function of borehole depth Z and compared to previous studies. Source: Mignan et al., 2019

Note that the amount of energy E considered for the above prices is larger but still close to the physical limit of how much electricity an EGS power plant can really generate. But it does so by considering an optimistic possible scenario, the scenario where

the flowrate V_{opt} causes no unintended induced seismicity, which can have significant effects to E. For example, experience has shown that seismicity is minimal when the reservoir overpressure does not exceed the minimum effective stress S_{hmin} anywhere in the reservoir. In these cases and considering the simple proxy suggested by Eaton (1969), where $S_{hmin} = P_h + \nu/(1-\nu)(S_v - P_h)$ and where P_h is the hydrostatic pressure, S_v the vertical stress and ν Poisson's ratio, then the flow rate might have to be capped at

$$V_{inj} = \min\left(V_{opt}, \frac{S_{\min}(1-3\sigma_S) - P_h}{I_{res}}\right), \tag{13}$$

in order to operate with a safety of at least 3 standard deviations σ_s. Energy revenue from the meta-model are going to be reduced by a factor of almost 4 if such a capping is forced in the triplet shown in Fig. 2 when σ_s is 10% of S_{hmin}.

Other less optimistic scenarios are not considered, as for example, a significant decline of ΔT with time or inclined wells, the drilling costs of which increase faster with the true vertical depth Z.

3. EFFECT OF INDUCED SEISMICITY IN THE ECONOMICS AND THE SITING OF EGS

The meta-model presented in section 2 allows quickly assessing a realistic lower limit for the price P_{EGS} when induced seismicity does not cause any issues. However, risk-based TLS are expected to be employed that will sometimes demand the premature termination of a well's stimulation due to high seismic risk for local infrastructures. Here, the meta-model is extended in estimating the probability p of an EGS well to be indefinitely abandoned due to a TLS's decision and in incorporating this probability in the LCOE of EGS.

3.1 Induced seismicity Risk Model

Here, the probability p of an EGS well to be indefinitely abandoned due to the decision of a traffic light system (TLS) is approximated by performing a probabilistic seismic assessment for the meta-model presented in section 2. The decision for prematurely ending a planned stimulation depends on the distance d of the EGS from the nearest habitation and is based on the Individual Risk (*IR)* (Broccardo et al., 2017a) there, i.e. the probability of a statistically representative individual dying within a given timeframe and at a given location (in micromorts [μmt]). The steps followed are:

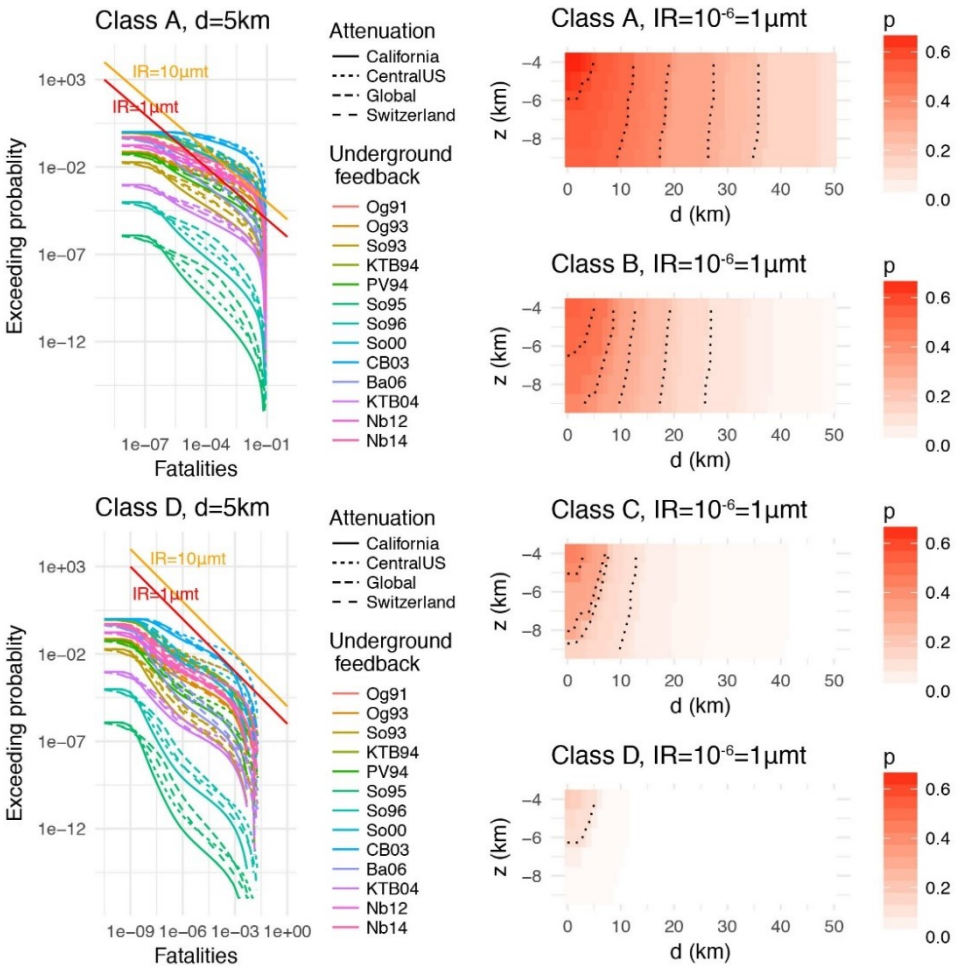

Figure 4: On the left, fatality risk curve scenarios are plotted for the reservoir stimulation phase, for a reservoir depth of *6* km and total injected volume 30,000 m³. On the right, the probability *p* of breaching a safety standard of *IR* = 1μmt is plotted as function of depth *Z*, distance from the nearest inhabitant *d*, and the same total injected volume. Source: Mignan et al., 2019

1. Probabilistic seismic hazard assessment (PSHA), where the probability of induced seismicity events with certain magnitude and intensity is assessed. The PSHA is based on a specific seismic risk rate model for fluid induced seismicity defined in Mignan et al. (2017) and Broccardo eta al. (2017a).

2. Probabilistic risk assessment (PRA), where the probability of certain damage and the corresponding expected fatality are estimated for the results from PSHA and for the known exposure.

3. Ascertaining whether the safety standard for *IR* is respected or not (*IR* based decision), where *IR* up to 1 μmt is well acceptable according to legislation.

For PSHA, the probability of exceeding a given intensity at any distance *d* from the EGS power plant is assessed. The number of earthquakes from many past EGS stimulations are re-normalized for a fixed total injected volume of *30,000* m^3 and a set of equally probable Guttenberg-Richter-like exponential distributions is obtained for each injected volume. The probability of the largest experienced induced magnitude is estimated out of these distributions for when the largest possible magnitude is truncated from the tectonic environment as suggested by van der Elst et al. (2016) and when it is truncated by the total injected volume as suggested by McGarr (2014). The probability of the largest magnitude is estimated by considering both truncations equally probable. Finally, for each possible largest magnitude the intensity *I* is estimated by averaging several empirical magnitude-intensity relationships that are all functions of the distance from the epicenter (Mignan et al., 2015) and the PSHA is concluded.

PRA is possible, once the probability of each intensity *I* has been assessed. For each intensity, the mean damaged grade $0 < \mu_D < 5$ is estimated for a building

$$\mu_D = 2.5\left[1+\tanh\left(\frac{I+6.25V_i-13.1}{2.3}\right)\right], \tag{14}$$

where ductility equals to *2.3* and V_i is the vulnerability, which V_i is a proxy to the EMS-98 classification as in Lagomarsino and Giovinazzi (2006) and it takes four discrete values (approximately $\{0.9, 0.75, 0.6, 0.4\}$), one for each of the four considered building classes: “class A” (e.g., adobe masonry), “class B” (e.g., simple stone masonry), “class C” (e.g., reinforced concrete without earthquake resistant design and “class D” (e.g. reinforced concrete with earthquake-resistant design). Also as in EMS-98, five discrete damaged grades are defined as follows: no damage (DG_0), slight (DG_1), moderate (DG_2), heavy (DG_3), very heavy (DG_4) and destruction (DG_5), and the probability of the *k*-th damage grade DG_k for a building follows the binomial distribution

$$p_k = \frac{5!}{k!(5-k)!}\left(\frac{\mu_D}{5}\right)^k\left(1-\frac{\mu_D}{5}\right)^{5-k}, k=\{0,1,2,3,4,5\} \tag{15}$$

PRA is completed by assuming an equivalent fatality rate equal to 10^{-5}, $2\cdot10^{-5}$, $2\cdot10^{-4}$, and *0.1* for damage grades DG_2, DG_3, DG_4, and DG_5, respectively (no fatalities assumed for DG_0 and DG_1). The practical outcome of the PRA are several fatality curves as shown in Fig. 4 that are functions of distance from the epicenter *d* for different underground seismic feedbacks.

Finally, the *IR*-based decision is reached simply by comparing the frequency with which fatality curves exceed a specified *IR* threshold for an EGS project, given the distance *d* from the nearest habitation and *30,000* m^3 of injected water considered for stimulating the EGS project.

Practically, by considering all possible intensity scenarios for the considered injected volume, the probability *p* is found as a function of the exposure and its distance *d*. Here, the probability of exceeding this *IR* threshold is also plotted in Fig. 4 and it coincides with the probability *p* of abandoning the well due to TLS protocol.

3.2 Cost of induced seismicity and behavioral decision-making energy model

When a TLS predicts excessive induced seismicity risk, then the EGS well might have to be abandoned. The probability of this scenario happening is *p* and is included in the LCOE here, with the fair price

$$P_{fair} = \frac{1}{E}\left[\frac{p}{1-p}C_{TLS}+C\right] = \frac{C_{TLS}}{E}\frac{p}{1-p}+P_{EGS}, \tag{16}$$

where as mentioned before $C_{TLS} = (C_{well} + C_{frac})$. This fair pricing P_{fair} weights C_{TLS} with a Bernoulli trial $p/(1-p)$, which makes the LCOE behave like a lottery.

However, and besides its undisputed importance, the probability *p* is deeply uncertain and highly subjective. Probability *p* is going to be assessed differently by each stakeholder for each project but also differently by the same stakeholder as the experience of the stakeholder increases. The Cumulative Prospect Theory (CPT) by Tversky and Kahneman (1992) is employed in the context of decision-making when faced with risks arising from induced seismicity (Goda and Hong, 2008), and the human factor in subjectively assessing *p* can be considered for the LCOE, in which case eq. (16) is generalized to

$$P_{averse} = \frac{1}{E}\left[\frac{p^\delta}{(1-p)^\gamma}\frac{\left(p^\gamma+(1-p)^\gamma\right)^{1/\gamma}}{\left(p^\delta+(1-p)^\delta\right)^{1/\delta}}\lambda C_{TLS}^\beta\right]^{1/\alpha}+P_{EGS}, \tag{17}$$

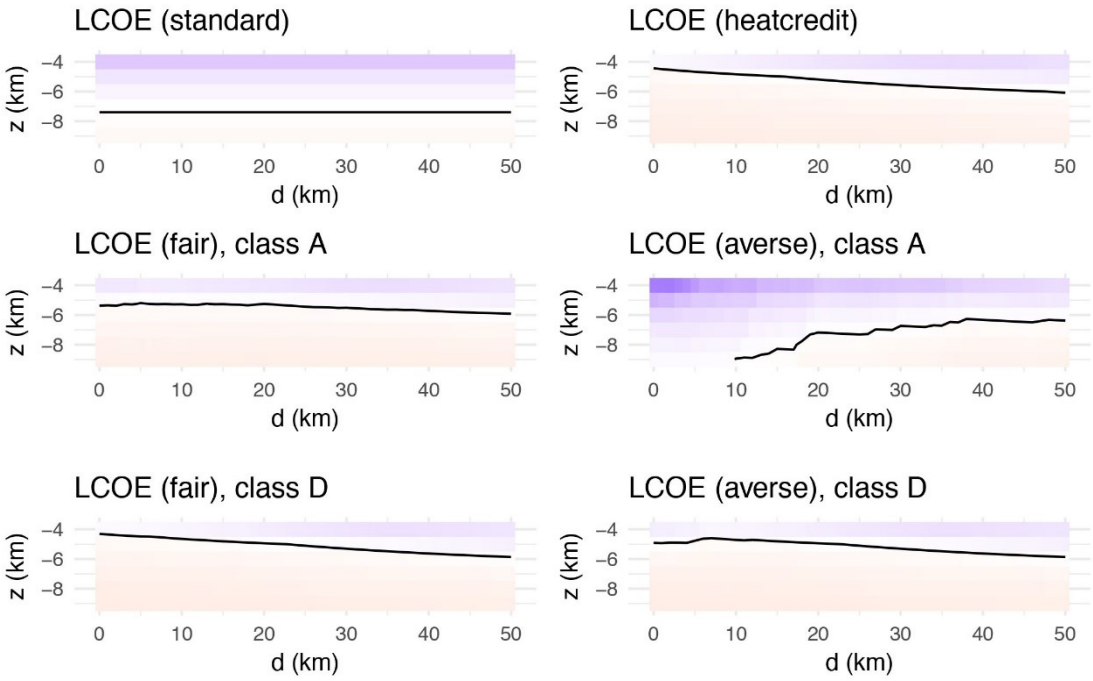

Figure 5: Different LCOE scenarios for V_{opt} and *IR = 1 µmt*. The black curve is the break-even price set at *6 ¢/kWh*, purple colour indicates too high prices and light red low enough. Source: Mignan et al., 2019

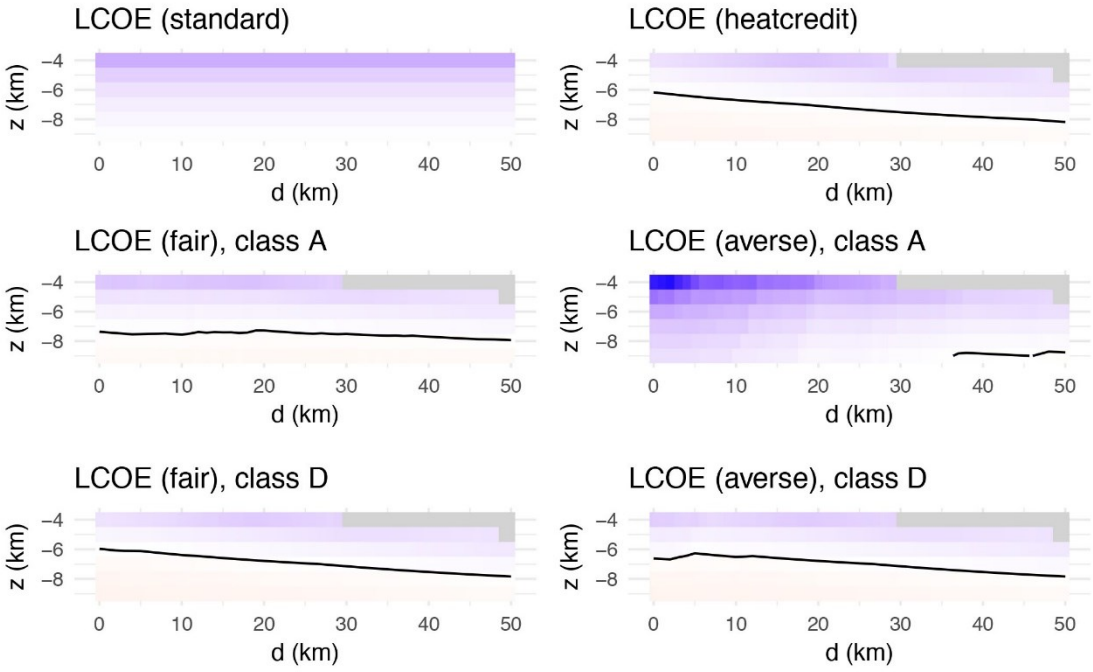

Figure 6: Different LCOE scenarios for the clipped *Vinj* and *IR=1µmt*. The black curve is the break-even price set at *6 ¢/kWh*, purple colour indicates too high prices and light red low enough. Source: Mignan et al., 2019

where $\alpha \leq \beta \leq 1 \leq \lambda$ are the coefficients of the selected value functions and $\gamma \leq \delta$ of the selected weighted functions for performing CPT. Mignan et al. (2019) adapted in their studies $\alpha = 0.78$, $\beta = 0.82$, $\lambda = 2.18$, $\gamma = 0.72$ and $\delta = 0.77$, which are the mean estimates of several CPT parameterizations previously considered by Booij et al. (2010). Practically, thanks to CPT the human inability of objectively assessing p and its consequences is introduced to the LCOE. In the present context, this leads to a risk-averse behavior and a further increase of the LCOE due to investor scare of potential, although low-probability, project failure.

In Figs. 5 and 6 the prices P_{EGS} with and without heat credit, as well as the price P_{fair} and P_{averse} both for very vulnerable buildings (class A) and very earthquake resilient buildings (class D) are plotted both for the optimal V_{opt} and the clipped rate of eq. (13), where the distance d and the distance L are considered equal. The importance of commercially exploiting the waste heat from an EGS is evident from comparing the two P_{EGS} prices for the V_{opt} scenario (Fig. 5); break even without heat-credit is only possible for very deep wells, but it can be achieved with 20-40% shallower wells if the waste heat can be exploited within a 50 km radius. Risk from induced seismicity should be affecting the latter P_{EGS} price only when the EGS is within a 20 km distance from very

vulnerable buildings, since P_{fair} is very close to P_{EGS} for longer distances or for earthquake resilient buildings. However, the price P_{fair} considers knowledge and rational decisions. The effect of the latter bias in the pricing is seen in the risk-averse LCOE case, where break-even is practically not to be expected when the EGS is less than 10 km from highly vulnerable buildings, a radius distance that disfavors LCOE even for EGS projects surrounded only by resilient buildings. When the least desired scenario of clipped rates due to excessive nuisance from operation-induced seismicity is considered (Fig. 6), then break-even is practically not feasible without exploiting the waste heat or when very vulnerable buildings are within the considered 50 km distance. When exposure is limited to resilient buildings, then break-even occurs in drillable depths and in meaningful distance from the exposed to risk buildings.

4. CASE STUDY: SITING OF EGS POWER PLANTS IN A FREE ENERGY MARKET

As shown in the previous sections, when the TLS constraint is neglected, then both the LCOE is significantly underestimated and the potential of EGS to be operated close to towns vulnerable to earthquakes is overestimated. On the other hand, the averse LCOE presented for EGS includes the cost from mitigating risk with a TLS and returns an optimal distance of EGS that is not right next to the towns. The averse LCOE allows estimating the total amount of energy that EGS can competitively provide and the potential of the technology in returning profits can be reassessed too, now that TLS are unavoidable.

Here, the potential of EGS is assessed for several random synthetic exposure datasets. All datasets consider scenarios of 10 towns scattered over a 100 km × 200 km region, the towns' sizes follow a power-law distribution, and only buildings of class B exist (e.g., simple stone masonry). A total of approx. 65,000 buildings are considered in all scenarios and buildings require on average 5kW.

Free-energy market is assumed but with a steady price of energy, where all buildings buy energy at 6 ¢/kWh and do not take the source of the energy into consideration (e.g. renewable or not). All players in the EGS market are aware of not only the town's locations and its exposure, but also expect the same temperature at 6 km depth everywhere. The rest of the rules are: 1) Potential EGS sites are only the ones with risk $IR \leq .1$ μmt and are occupied on a first-come-first-served basis, 2) an EGS can sell heat only to its closest town, and 3) there should be at most one EGS site for each town that operates with exactly $IR = 1$ μmt (to avoid seismic risk accumulation).

For each sampled exposure dataset, the potential sites are only those abiding by the rules and with price $P_{averse} \leq 6$ ¢/kWh. Initially, the site with the least P_{averse} is occupied first, and the list of potential sites is updated before the step is repeated and the next EGS site is chosen. Without loss of generality, the same EGS power plant is always considered that generates 10 MW.

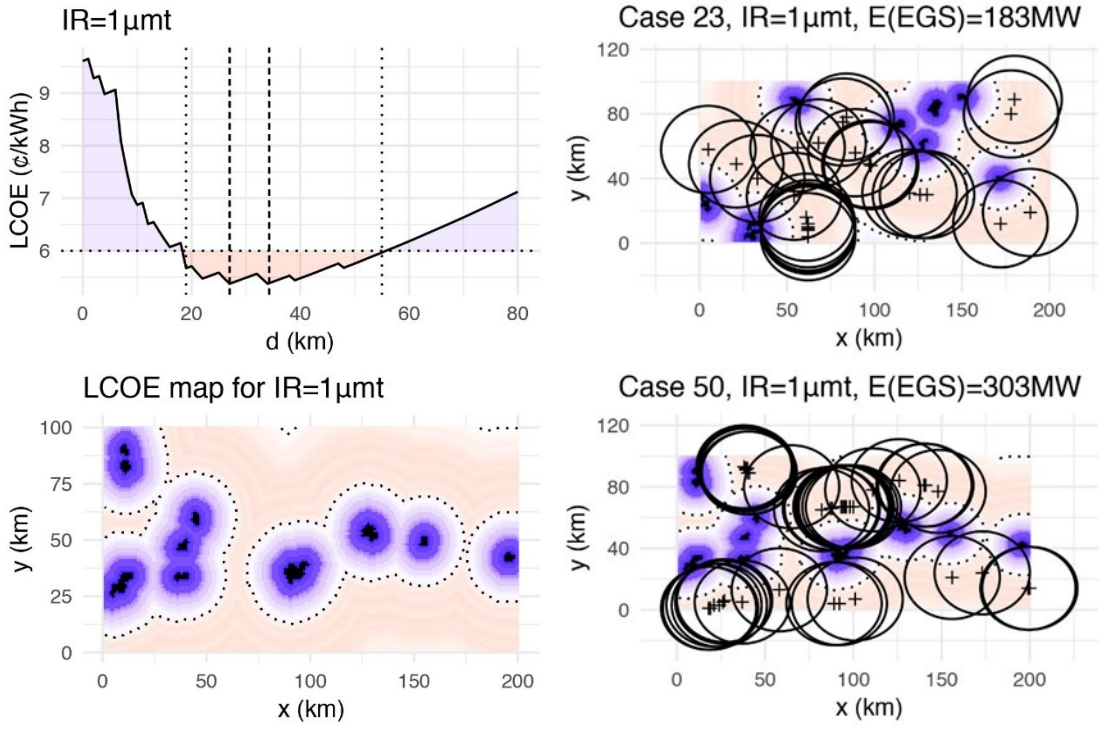

Figure 7: On the left, the considered averse LCOE and its spatial distribution for a synthetic case are plotted, and on the right the resulting siting of EGS power plants for two different synthetic cases.

In Fig. 7, the averse LCOE of the considered EGS power plant is plotted as a function both of distance d from one building and of minimum distance d on a synthetic exposure dataset with no individual buildings but with towns. Clearly, only EGS within 20-60 km distance from a town can be profitable for the considered EGS power plant, and profit is possible only outside of the dashed limits surrounding the towns (dark black locations). Also in Fig. 7, the siting of EGS power plants in the considered free market is plotted for two different cases. Despite the fact that both cases follow the same statistical distributions and need for approx. 320 MW of energy, the adverse LCOE and the meta-model imply that only one of the two exposures can indeed cover most of its need only with EGS technology. The other case is going to require access to different sources of energy for more than 40% of its needs.

Obviously, increasing the acceptable risk (i.e. increasing the *IR* threshold) would mean increased EGS energy potential at the detriment of public safety (see examples given in Mignan et al., 2019).

5. CONCLUSION AND RECOMMENDATIONS

The impact of risk mitigation measures to the price of EGS and to their share in the competitive market was shown and studied here.

Based on a meta-model for assessing the price of EGS, it was reaffirmed that cogenerating electricity and heat with an EGS have a significant effect on the price of EGS. Siting EGS power plants next to urban environments is not any more found to be the most competitive case since EGS power plants sited at a distance of at least 5 km from inhabited buildings are found to be always a scenario with more competitive price due to decreased seismic risk with distance from the plant. Both the minimum LCOE and its distance from buildings increase as the vulnerability of the buildings increases.

By mimicking a free energy market, it is shown that the expected share of EGS in the energy mix is going to be limited by the spacing between vulnerable regions. Realistic assessments of the technology's potential share in the energy market require sufficient knowledge of the exposure. Also by mimicking the free market, individual buildings can be pointed, to the vulnerability of which the competitiveness of an EGS project is sensitive. Given that the necessity of risk mitigation measures like the use of a TLS is undisputable, simple solutions like retrofitting these buildings could significantly improve the overall LCOE from EGS.

Besides TLS, the LCOE of EGS can be significantly increased also by unintended induced seismicity occurring during the operation of the EGS. In this case, the flow rate is going to be capped, in order to reduce the pressures inside the reservoir, which capping is going to significantly increase the LCOE. This scenario can be avoided mainly through achieving an EGS with a very low impedance between its wells, (e.g. multi-staged stimulation).

Last but not least, the competitiveness of EGS seems to rely heavily on insulated pipes that can supply heat to long distanced district heating systems. That long insulated pipelines for heating exist but they are very few. Here, their costs have been oversimplified. Moreover, we have neglected potentially important gains and costs, which actually depend mostly on the actual path of the pipe on a certain landscape, and instead, the same scenario is considered for all pipeline costs that is most likely not the optimal. More accurate assessments of the EGS costs for heating should include the heat gain from the frictional losses due to the turbulent flow in the supply pump, the electricity costs for compensating these frictional losses with a pump, the thermosiphon effect, and the expected saving of costs by several EGS using the same pipelines, since the spacing of exposure promotes the clustering of EGS power plants (Fig. 7).

FUNDING

This work was supported by the Swiss Competence Center for Energy Research – Supply of Electricity (SCCER-SoE).

REFERENCES

Amann, F., Gischig, V., Evans, K., Doetsch, J., Jalali, R., Valley, B., … Giardini, D. (2018). The seismo-hydromechanical behavior during deep geothermal reservoir stimulations: open questions tackled in a decameter-scale in situ stimulation experiment. Solid Earth, 9(1), 115–137. doi: 10.5194/se-9-115-2018

Andrae, A., & Edler, T. (2015). On Global Electricity Usage of Communication Technology: Trends to 2030. Challenges, 6(1), 117–157. doi: 10.3390/challe6010117

Baker, J. W. and A. Gupta (2016), Bayesian Treatment of Induced Seismicity in Probabilistic Seismic-Hazard Analysis, Bull. Seismol. Soc. Am., 106, 860-870, doi: 10.1785/0120150258

Beckers, K. F., M. Z. Lukawski, B. J. Anderson, M. C. Moore and J. W. Tester (2014), Levelized costs of electricity and direct-use heat from Enhanced Geothermal Systems, J. Renewable and Sustainable Energy, 6, 013141, doi: 10.1063/1.4865575

Bertani, R. (2012). Geothermal power generation in the world 2005–2010 update report. Geothermics, 41, 1–29. doi: 10.1016/j.geothermics.2011.10.001

Bertani, R. (2016). Geothermal power generation in the world 2010–2014 update report. Geothermics, 60, 31–43. doi: 10.1016/j.geothermics.2015.11.003

Booij, A. S., B. M. S. van Praag and G. van de Kuilen (2010), A parametric analysis of prospect theory's functionals for the general population, Theory Dec., 68, 115-148, doi: 10.1007/s11238-009-9144-4

Broccardo, M., Danciu, L., Stojadinovic, B., and Wiemer, S. (2017a). Individual and societal risk metrics as parts of a risk governance framework for induced seismicity. In *16th World Conference on Earthquake Engineering (WCEE16).*

Broccardo, M., Mignan, A., Wiemer, S., Stojadinovic, B., & Giardini, D. (2017b). Hierarchical Bayesian Modeling of Fluid-Induced Seismicity. Geophysical Research Letters, 44(22), 11-357. doi: 0.1002/2017GL075251

Eaton, B. A. (1969), Fracture Gradient Prediction and Its Application in Oilfield Operations, Journal of Petroleum Technology, 21, 1353-1360

Edwards, B., T. Kraft, C. Cauzzi, P. Kastli, & S. Wiemer (2015), Seismic monitoring and analysis of deep geothermal projects in St Gallen and Basel, Switzerland, Geophys. J. Int., 201, 1022-1039, doi: 10.1093/gji/ggv059

Giardini, D. (2009). Geothermal quake risks must be faced. Nature, 462(7275), 848–849. doi: 10.1038/462848a

Goda, K. and H. P. Hong (2008), Application of cumulative prospect theory: Implied seismic design preference, Structural Safety, 30, 506-516, doi: 10.1016/j.strusafe.2007.09.007

Hirschberg, S., S. Wiemer and P. Burgherr, eds. (2015), Energy from the Earth, Deep Geothermal as a Resource for the Future?, Centre for Technology Assessment, TA Swiss, 447 pp., doi: 10.3218/3655-8

Kneafsey, T. J., Dobson, P. F., Ajo-Franklin, J. B., Valladao, C., Blankenship, D. A., Knox, H. A., … Zoback, M. D. (2018). The EGS collab project: Stimulation and simulation. 52nd U.S. Rock Mechanics/Geomechanics Symposium.

Lagomarsino, S. and S. Giovinazzi (2006), Macroseismic and mechanical models for the vulnerability and damage assessment of current buildings, Bull. Earthquake Eng., 4, 415-443, doi: 10.1007/s10518-006-9024-z

Lee, K.-K., Ellsworth, W. L., Giardini, D., Townend, J., Ge, S., Shimamoto, T., … Langenbruch, C. (2019). Managing injection-induced seismic risks. Science, 364(6442), 730–732. doi: 10.1126/science.aax1878

McGarr, A. (2014), Maximum magnitude earthquakes induced by fluid injection, J. Geophys. Res. Solid Earth, 119, 1008-1019, doi: 10.1002/2013JB010597

Mignan, A., D. Landtwing, P. Kästli, B. Mena and S. Wiemer (2015), Induced seismicity risk analysis of the 2006 Basel, Switzerland, Enhanced Geothermal System project: Influence of uncertainties on risk mitigation, Geothermics, 53, 133-146, doi: 10.1016/j.geothermics.2014.05.007

Mignan, A., Broccardo, M., Wiemer, S., & Giardini, D. (2017). Induced seismicity closed-form traffic light system for actuarial decision-making during deep fluid injections. Scientific reports, 7(1), 13607. doi: 10.1038/s41598-017-13585-9

Mignan, A., M. Broccardo, S. Wiemer, & D. Giardini (2019), Autonomous Decision-Making Against Induced Seismicity in Deep Fluid Injections, In: Ferrari, A., & L. Laloui (eds.), Energy Geothenics, SEG 2018, Springer Series in Geomechanics and Geoengineering, 369-376, doi: 10.1007/978-3-319-99670-7_46

Mignan, A., Karvounis, D., Broccardo, M., Wiemer, S., & Giardini, D. (2019). Including seismic risk mitigation measures into the Levelized Cost Of Electricity in enhanced geothermal systems for optimal siting. Applied Energy, 238, 831–850. doi: 10.1016/j.apenergy.2019.01.109

MIT (2006), The Future of Geothermal Energy, Impact of Enhanced Geothermal Systems (EGS) on the United States in the 21st Century, Massachusetts Institute of Technology, ISBN: 0-615-13438-6

Tester, J. W., et al. (2007), Impact of enhanced geothermal systems on US energy supply in the twenty-first century, Phil. Trans. R. Soc. A, 365, 1057-1094, doi: 10.1098/rsta.2006.1964

Tversky, A. and D. Kahneman (1992), Advances in Prospect Theory: Cumulative Representation of Uncertainty, J. Risk and Uncertainty, 5, 297-323

van der Elst, N. J., Page, M. T., Weiser, D. A., Goebel, T. H. W., & Hosseini, S. M. (2016). Induced earthquake magnitudes are as large as (statistically) expected. Journal of Geophysical Research: Solid Earth, 121(6), 4575–4590. doi: 10.1002/2016JB012818

Zarrouk, S. J. and H. Moon (2014), Efficiency of geothermal power plants: A worldwide review, Geothermics, 51, 142-153, doi: 10.1016/j.geothermics.2013.11.001